In: Remote Sensing: Techniques, Applications and Technologies ISBN: 978-1-62417-145-1
Editor: Enner Alcântara

Chapter 1

LAND-BASED REMOTE SENSING OF COASTAL BASINS: USE OF AN HF RADAR TO INVESTIGATE SURFACE DYNAMICS AND TRANSPORT PROCESSES IN THE GULF OF NAPLES

Daniela Cianelli[1,2], Marco Uttieri[1], Raffaele Guida[1], Milena Menna[3], Berardino Buonocore[1], Pierpaolo Falco[1], Giovanni Zambardino[1] and Enrico Zambianchi[1]

[1]Università degli Studi di Napoli "Parthenope", Dipartimento di Scienze per l'Ambiente, Centro Direzionale Isola C4, Napoli, Italy
[2]Istituto Superiore per la Protezione e la Ricerca Ambientale,Via Vitaliano Brancati 48Roma, Italy
[3]IstitutoNazionale di Oceanografia e Geofisica Sperimentale, Borgo Grotta Gigante 42/C, Sgonico (TS), Italy

ABSTRACT

Here, the results of an investigation that was performed on the surface dynamics of a coastal area using data provided by a land-based remote sensing system, a HF coastal radar, are presented. The surface circulation in the Gulf of Naples (southern Tyrrhenian Sea, western Mediterranean), as determined using measurements collected by a HF radar, displayed recurrent dynamics directly linked to prevailing forcing conditions. In this contribution we examine the circulation-dependent surface transport of passive particles released in a coastal sub-basin (Bay of Naples), as characterized by severe anthropic pressure. HF radar data from surface circulation were integrated using a transport model, and simulations of coastal-offshore transport were performed in order to estimate the residence times of the particles and to identify possible areas of retention and aggregation. Four test cases, representative of the most frequent seasonal observed circulation structures, were investigated. Depending on the forcing factor driving surface circulation, the results emphasized the existence of unique mechanisms.

1. INTRODUCTION

The subtitle of Ian Robinson's most recent book "Discovering the Oceans from Space" (2010) reads "The Unique Applications of Satellite Oceanography". The main aspect of uniqueness is the capability of remote sensing techniques to provide synoptic (i.e. simultaneous, over a broad area) measurements of physical and biological quantities within the upper layers of the ocean. If taking synoptic snapshots can only be obtained from a distance (*in situ* measurements are, by definition, not synoptic unless massive arrays of sensors are employed, which in the ocean has proved not to be feasible in logistic or economic terms), the possibilities are not only limited to satellite remote sensing. As early envisioned by Sherman (1969 and 1978), broader synoptic coverage can be fulfilled by aircraft-mounted, as well as by ship- or land-based oceanographic sensors.

Over the last two decades interest has arisen in HF coastal radars, a type of land-based remote sensing system that provides high spatial and temporal resolution measurements of surface currents in coastal basins. The availability of synoptic current measurements not only allows detailed studies of ocean circulation, but may also provide advective fields for models that predict the transport of pollutants or trajectories in search and rescue operations.

The history of land-based HF radar applications for ocean current mapping spans more than four decades. Since HF radar applications were designed for military purposes (mainly for detecting hard targets: ships, aircraft and missiles, and even Kelvin wakes from ships), the origin of the use of such oceanographic equipment for this purpose is almost accidental. The HF radar systems of the past were very bulky and extremely expensive to operate, and were characterized by very strong background noise due to backscattering from the sea surface (for strategic reasons they were typically installed in coastal regions). A breakthrough occurred when the perspective was inverted, and people began to consider backscattering from the sea surface as the signal rather than noise (Pederson and Barrick, 2004). Technology developments have allowed antenna downsizing (the original antennas installed by Don Barrick on San Clemente Island in 1970 were 500 m long!) and systems are now extremely compact, allowing for very easy installation in diverse coastal settings. As a result, the number of systems installed along the ocean's coasts has only strongly increased over the last 10-20 years (Harlan et al., 2010). Here, we demonstrate and exploit the capabilities of a HF coastal radar installed in the Gulf of Naples, a marginal basin of the southern Tyrrhenian Sea (western Mediterranean Sea).

Historical reports on the circulation of the Gulf of Naples (henceforth GoN) highlight the occurrence of highly dynamic structures over the basin (Moretti et al., 1976-1977 and 1983; De Maio et al., 1985; Cianelli et al., 2012; and for a recent assessment of summer circulation in the GoN see Uttieri et al., 2011). As for other marginal and coastal basins, even in GoN, wind stress represents the most important local forcing, directly and indirectly – e.g., through interactions with local orography and bottom topography - affecting surface current fields, as evident from both empirical and modelling results (Moretti et al., 1976-1977; De Maio et al., 1985; Gravili et al., 2001; Grieco et al., 2005; Menna et al., 2007; Cianelli et al, 2012). Wind forcing displays a typical seasonality (Menna et al., 2007; Uttieri et al., 2011) that is associated with the large-scale atmospheric circulation acting over the region. When such forcing is weak, as often in summer, a locally induced breeze regime can act as the primary driver of sea surface circulation.

The circulation of the GoN can also be remotely driven by the larger-scale circulation of the southern Tyrrhenian Sea (Gravili et al., 2001), which it is in communication with through the “Bocca Grande” and “Bocca Piccola” apertures (Figure 1). The Tyrrhenian circulation has a marked barotropic component (Pierini and Simioli, 1998) and is basically organized in three main gyres (two cyclonic and a central anticyclonic) with typical seasonal patterns (Artale et al., 1994). Recent observations from surface drifters and satellite altimetry (Rinaldi et al., 2010) have shown that circulation in the southern Tyrrhenian Sea is extremely complex, and only in a very broad sense can be considered as “overall cyclonic” (e.g., Millot, 1999). However, it is modulated by a series of mesoscale/subbasin structures, of both a transient and semi-permanent nature. The importance of these structures overcomes the mean flow. However, during winter an intense northward flow may develop along the eastern Tyrrhenian coast, as supported by the intrusion of Modified Atlantic Water (Krivosheya and Ovchinnikov, 1973), resulting in a coastal current that represents the main remote forcing of the circulation in the interior of the GoN.

In addition to its unique hydrographic and oceanographic features, for socio-economic reasons the GoN has a leading role among marginal basins of the southern Tyrrhenian Sea. Severe anthropic activity impinges the area and ranges from urban settlements to tourism and maritime traffic that can have drastic consequences on ecosystem dynamics and water quality. The necessity of preserving and sustainably exploiting environmental resources requires an accurate understanding and the monitoring of circulation and transport processes acting within the basin, by forestalling or mitigating potentially hazardous events. In recent years, increasing awareness regarding the importance of operational oceanography systems (e.g., Flemming et al., 2002; Dahlin et al., 2003) has promoted the development of new techniques and instruments to investigate real-time, multi-scale circulation patterns in a target area as well as their effects on transport and pollutant diffusion, with a special emphasis on coastal zone management.

The purpose of this work was to study surface circulation patterns within the GoN as driven by typical local wind conditions and by southern Tyrrhenian guidance, and to assess their effects on the transport processes of passively buoyant particles. The synoptic, basin-scale circulation of the GoN was reconstructed using a HF radar system that has been operating since October 2004. From the available dataset we selected four periods, each lasting one week, with typical forcing conditions (section 2). For each period we investigated the associated surface current velocity and the vorticity fields (section 3). Thereafter, to simulate the fate of passive conservative particles released in a coastal sub-area, the Bay of Naples (section 4), we applied a transport model. The results presented here indicate that each set of conditions determined unique circulation structures and transport processes, as the result of the superimposition of multiple co-occurring factors. Such an integrated approach, recently utilized for the study of a very specific pollution event in the area (Uttieri et al., 2011), allowed an evaluation of surface water renewal times and investigations regarding exchange mechanisms between sub-basins.

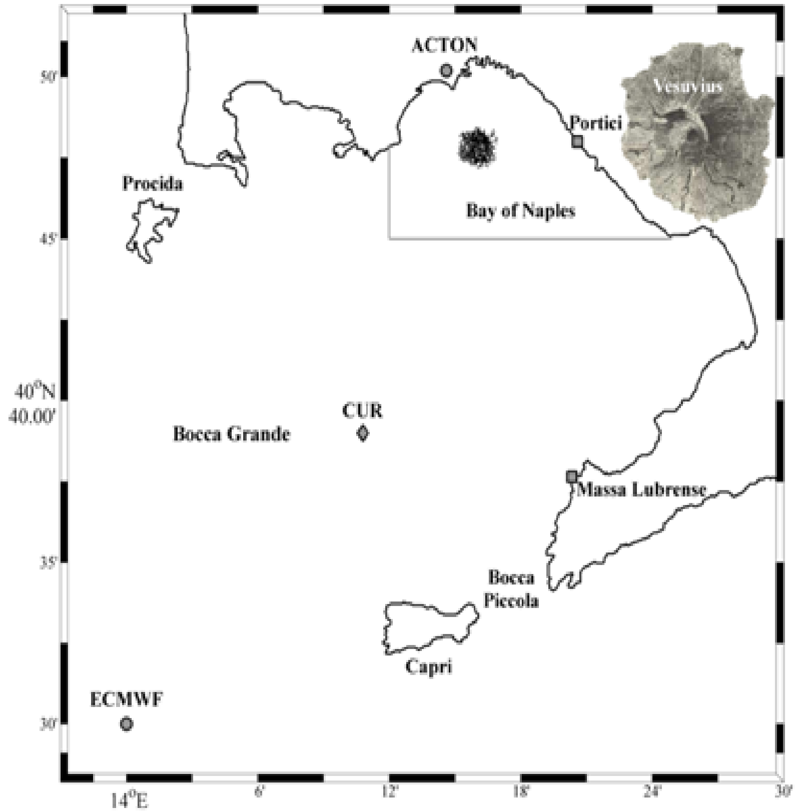

Figure 1. A map of the Gulf of Naples (southern Tyrrhenian Sea), within the location of the two radar antennas whose data were used in this work (Portici and Massa Lubrense), for the DiSAm Acton weather station, the ECMWF grid point and the point where currents were evaluated in the breeze regime case (CUR, see Figure 4).

2. Local and Remote Forcings of the Surface Circulation

The analysis of local wind forcing was performed using the meteorological data set recorded by a weather station located in the urban area of Naples (Acton station: 40° 30'.19 N, 14° 15'.21 E). The station belongs to the monitoring network managed by the Department of Environmental Sciences at Parthenope University (DiSAm). To compare small-scale with basin-scale wind features, data relative to the closest gridpoint (40° 30'.00 N, 14° 00'.00 E) of the operational weather forecast model of the European Centre for Medium-Range Weather Forecasts (ECMWF) were also analyzed (Figure 1). The Acton station and ECMWF data were in good agreement; only in cases of southwesterly wind ECMWF recordings was a shift in direction determined, most likely due to the position of the Acton station which, owing to orographic barriers, is sheltered from westerly winds (Menna et al., 2007).

Interannual investigations over the 2002-2006 period (Menna et al., 2007) indicated the occurrence of two prevailing wind directions, one from the NE-NNE and one from the SW-

SSW, in direct association with large-scale meteorological dynamics. When these large-scale forcings are weak, as often recorded during summer, a breeze regime arises and winds blow from the sea to land during the day and from land to sea during the evening. The breeze regime can also be observed during other periods of the year, typically in correspondence to passages of high pressure centers within the GoN.

Using these results, we selected three characteristic periods from the available data set, each lasting one week, during which the wind field maintained marked directional stability. The chosen time span allowed us to analyze the formation and the development of the surface circulation structures associated with different forcing conditions, as follows:

- *The LND case study:* winds from the NE (Figure 2a). The selected period corresponded to November 1-8 2007, with wind intensities in the range 2-6 m s^{-1} and occasional gusts ≥ 8 m s^{-1}.
- *The SEA case study:* winds from the SW (Figure 3a). The selected period for this condition was January 17-24, 2007. The stick diagram in Figure 3a shows wind velocities in the range 2-6 m s^{-1}, with occasional gusts ≥ 12 m s^{-1}.
- *The BRZ case study:* the breeze regime (Figure 4a). The selected period for this situation was August 1-8, 2007. The stick diagram shows alternating wind directions approximately every 12 hours with lower intensities than in the previous cases (0-6 m s^{-1}).

In addition to the three case studies discussed above, we also investigated surface circulation as directly guided by a current in the neighbouring southern Tyrrhenian Sea. Preliminary investigations (De Maio et al., 1983; Cianelli et al., 2012) indicated that the direct effect of the southern Tyrrhenian is manifested through the development of an intense jet aligned along the Capri/Ischia direction, enhancing the intrusion of Tyrrhenian waters into the GoN. The result is supported by the analysis of trajectories of drifting buoys launched in the southern Tyrrhenian and entering the basin (Rinaldi et al., 2010). Therefore, in this work we also present the following fourth case:

- *The TYR case study:* southern Tyrrhenian forcing (Figure 5a). The period selected was December 10-17, 2006. At this time of the year the southern Tyrrhenian circulation displays an intense northward flux (Artale et al., 1994; Pierini and Simioli, 1998). The recordings for the selected period show intense south-easterly winds, with occasional changes in direction.

3. Surface Dynamics As Detected by a Land-Based HF Coastal Radar

The acronym RADAR (RAdio Detection And Ranging) defines an apparatus that sends an electromagnetic signal, typically within the range of microwaves, toward a target and receives its backscattered echo. From the time lag between transmission and reception it is possible to calculate the target distance.

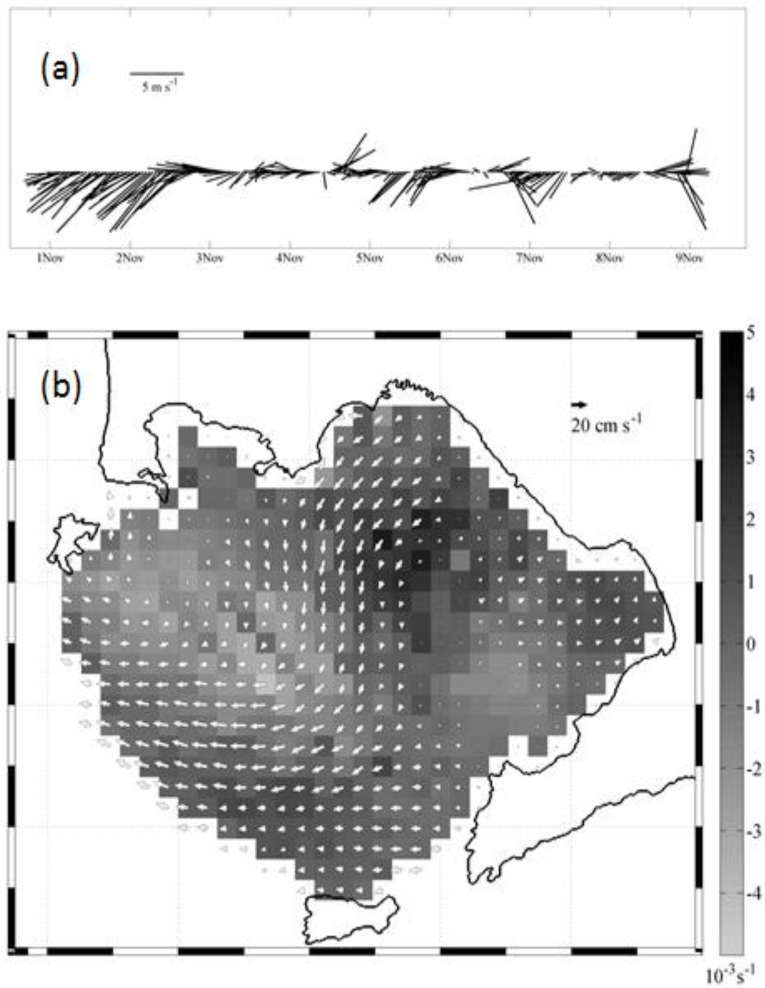

Figure 2. The LND case study: **(a)** a stick diagram for Acton wind data; **(b)** a surface current and vorticity map (Figure 2b refers to the circulation observed on Nov 5th, 2007, at 16:00 GMT).

For a coastal radar the target is represented by the crests and troughs of the gravity waves propagating at the surface of a coastal basin. The applicability to such a system is a consequence of Bragg scattering, originally conceived to explain the diffraction of X rays by a crystalline lattice, which can be applied to a sea surface perturbed by the presence of gravity waves.

The sea surface may act as a diffraction grating for the electromagnetic signal at a suitable wavelength. The backscattered radiation will be in a condition of constructive interference when the wavelength of the sea surface roughness is approximately half the wavelength of the incoming signal.

The gravity waves that develop in coastal basins have relatively universal characteristics. Therefore, the operational frequency of coastal radar is typically within a range that optimizes the probability of backscattering by surface waves. The choice of operating frequencies for individual systems can be determined by considering its sought-after range and resolution.

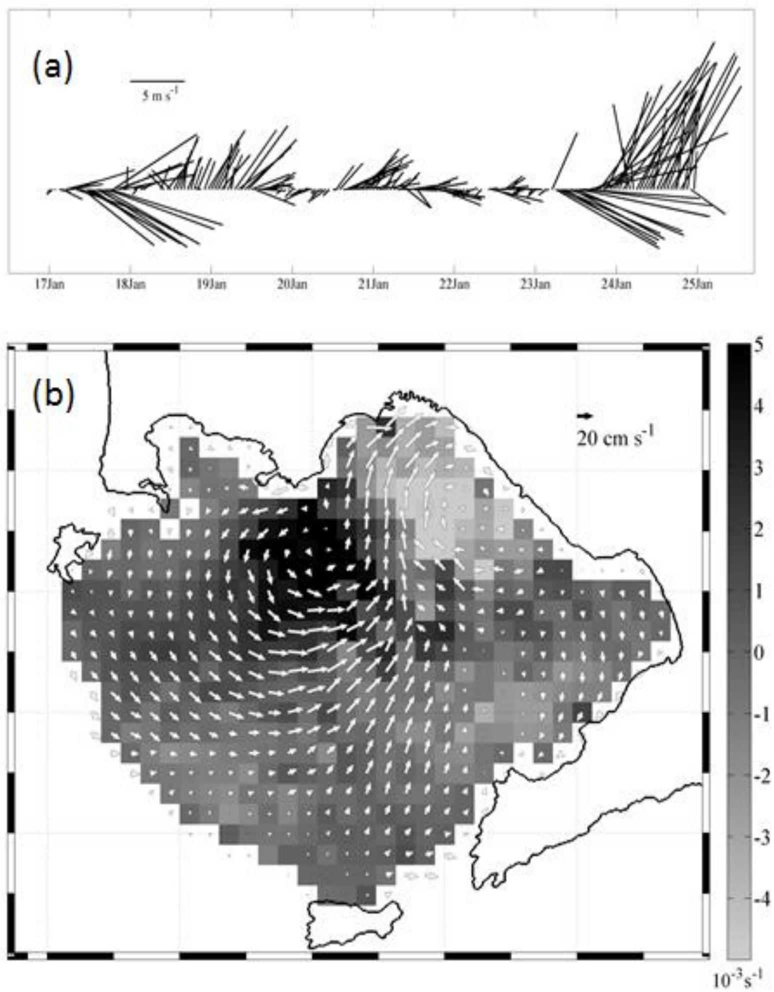

Figure 3. The SEA case study: **(a)** a stick diagram for Acton wind data;**(b)** a surface current and vorticity map (Figure 3b refers to the circulation observed on Jan 17th, 2007, at 18:00 GMT).

If the surface gravity waves responsible for backscattering are stationary waves, the signal received from each station will have the theoretical characteristics described above. However, in reality waves are almost never stationary, and propagate toward or away from the antenna location; yielding a frequency variation for the received signal, due to the Doppler effect, that causes a frequency increase for approaching wave trains and a decrease for retracting ones.

If waves are superimposed onto a surface current field, the frequency of the backscattered signal is characterized by an additional Doppler shift that is induced by the radial (approaching or retracted from the receiving station) component of the current (Barrick et al., 1977) that can be utilized to evaluate the current. When at least two transceiving stations are available, it is possible to combine their radial information on surface currents and to obtain a vector current field (Barrick and Lipa, 1986). Exhaustive reviews on HF radar principles and functioning can be found in Paduan and Graber (1997) and Teague et al. (1997).

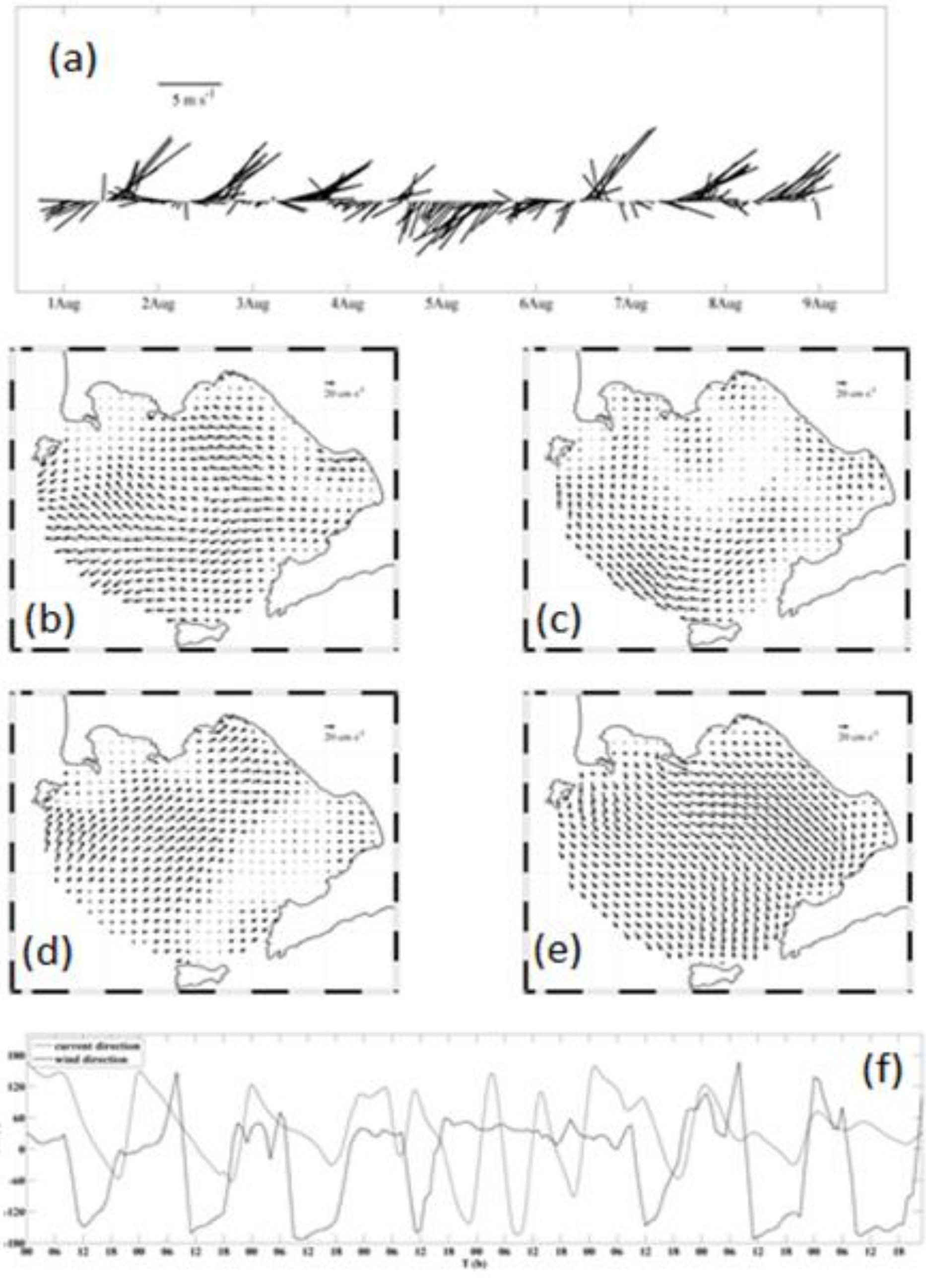

Figure 4. The BRZ case study: **(a)** a stick diagram for Acton wind data; **(b-e)** surface currents measured on Aug 1st, 2006, at 00:00, 06:00, 12:00, 18:00 GMT respectively; **(f)** the wind and current (measured at point CUR as shown in Figure 1) direction.

The synoptic surface circulation in the GoN was analyzed using data provided by a HF coastal radar (a SeaSonde system, manufactured by CODAR O.S. of Mountain View, California) that has been operated in the area since 2004 by the DiSAm on behalf of the AMRA consortium (where AMRA stands for the Analysis and Monitoring of Environmental Risks).

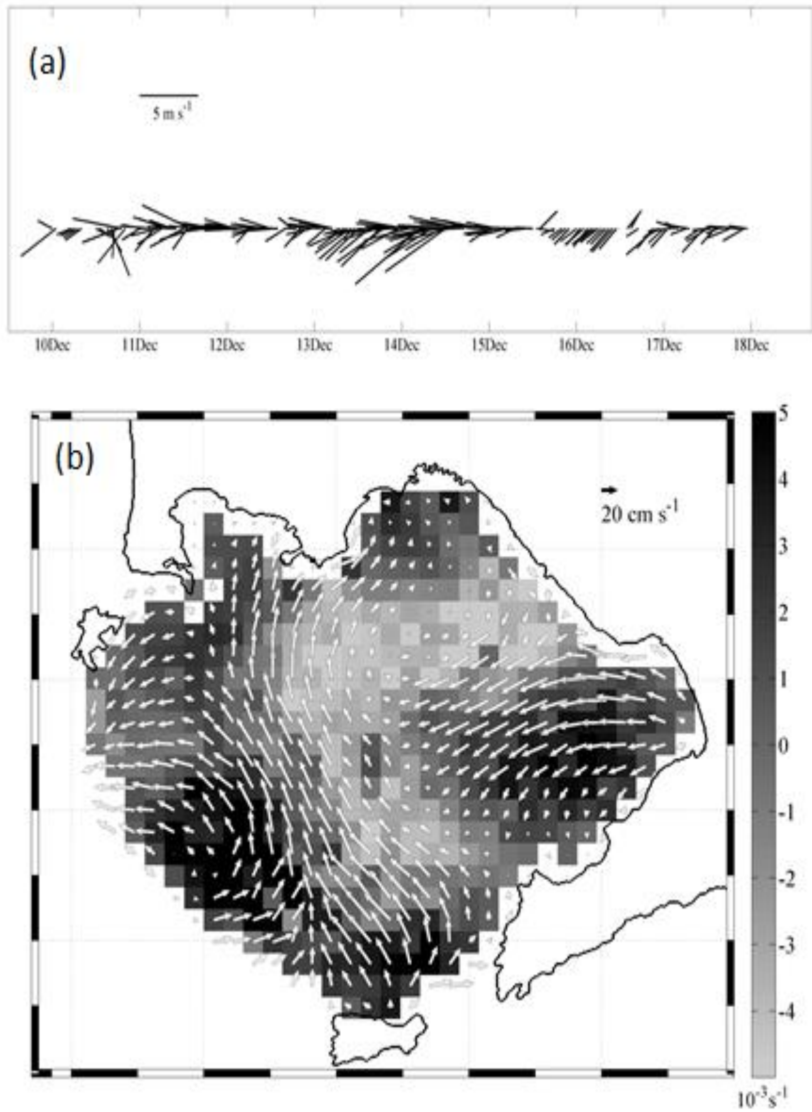

Figure 5. The TYR case study: **(a)** a stick diagram for Acton wind data;**(b)** a surface current and vorticity map (Figure 5b refers to the circulation observed on Dec 17^{th}, 2006, at 09:00 GMT).

The data presented in this work refers to the network configuration active until 2008, composed of two monostatic, direction-finding systems with three-element crossed loop/monopole antenna used to transmit and receive signals. To determine the bearing of an incoming signal, the directional properties of the antennas are exploited and a variant of the multiple signal classification algorithm is applied (MUSIC, see Schmidt, 1986).

Antennas were located in Portici and Massa Lubrense, while the central site for data processing and merging was hosted at DiSAm headquarters. The nominal operating frequency of the systems was 25 Mhz, and provided hourly data with a 1.250 km spatial resolution (the technical specifications of the utilized system are provided in Table 1; Figure 1 shows the antenna locations; a third antenna at Castellammare has recently been added, bringing the resolution to 1 km).

Table 1. The technical specifications of the HF radar system installed in the Gulf of Naples

RADIAL MAP ACQUISITION	
Frequency	25 Mhz
Sweep Rate	2.01 Hz
Samples per Sweep	2048
Band Width	150.147 Khz
Range Step	0.999 km
Range	~ 30.0 km
Wavelength	12 m
RADIAL MAP COMBINE OPTIONS	
Grid Spacing	1.250 km
Averaging Radius	2.0 km
Distance Angular Limit	25° GDOP limit
Current Velocity Limit	80 cm s^{-1}

Coastal radar coverage is often impacted by spatial and/or temporal gaps (see, e.g., Paduan and Cook, 1997). In particular, due to the presence of the Saracen tower in the immediate vicinity of the Massa Lubrense antenna, our system had a blind region in the southeastern portion of the GoN. For this reason, to interpolate the data in space so as to fill the no-data region with geometrical/dynamical methods, an Open-boundary Mode Analysis (OMA) procedure (Lekien et al., 2004) was adopted.

The OMA is an evolution of the Normal Mode Analysis (NMA) method introduced in the study of coastal circulation by Lipphardt et al. (2000), and represents its improvement in terms of the representation of the flow at open boundaries. Both the OMA and NMA are spectral objective mapping techniques that use two subsets of functions (vorticity modes and divergence modes) to represent a velocity field. The functions exactly enforce a no normal flow condition at the domain's solid boundaries and use a separate inhomogeneous open boundary solution to account for specified normal flow through the domain's open boundaries. The functions produce maps that are precisely consistent with a three-dimensional incompressible velocity field (the method can be extended to use 3D mapping functions to directly map 3D velocity data sets that are dense enough to properly constrain the mapping).

CODAR current data have also been used to reconstruct the vorticity field associated with surface circulation by means of the relative vorticity (ζ) evaluated as the vertical component of the curl of the velocity field (Pedlosky, 1979), as follows:

$$\zeta = (\vec{\nabla} \times \vec{v})_z = \frac{\partial v}{\partial x} - \frac{\partial u}{\partial y}.$$

In the following, we briefly describe the circulation observed in the GoN for the four case studies.

The LND case study: In the presence of winds from the NE, surface currents (Figure 2b) are roughly oriented along the E-W direction and describe a jet (mean velocity ~ 30 cm s^{-1}) in the central-southern region of the basin that is flanked by cyclonic and anticyclonic vorticity structures. The occurrence of the coastal jet as typically associated with northeasterly winds has been observed in the past using experimental data (Moretti et al., 1976-1977; Menna et al., 2007), as well as in model results (Gravili et al., 2001; Grieco et al., 2005).

The SEA case study: For SW wind conditions a coastward flux develops from the Island of Capri to the coast and to the Bay of Naples, with the formation of a persistent cyclonic gyre in the offshore sector of the GoN and the presence of other recirculation structures (both cyclonic and anticyclonic) at the basin and sub-basin scale (Figure 3b). Toward the end of the investigated period, the gyre progressively reduced its intensity until it disappeared, while a net coastward current spread over the entire basin. The results are in full agreement with previous observations (Menna et al., 2007) and confirm the numerical simulations of Gravili et al. (2001) and Grieco et al. (2005).

The BRZ case study: During the breeze regime, surface currents respond to wind stress with a periodic oscillation; the surface current pattern makes a 360° clockwise rotation within 24 hrs (Figures 4b-f). The wind intensity follows a daily breeze trend: the highest intensity was reached each day around h 12:00-13:00, while the lowest intensity was reached during night hours around midnight.

The TYR case study: For this case surface circulation in the GoN is guided by Tyrrhenian input that penetrates from the “Bocca Piccola” and partially from the “Bocca Grande”, as also verified by drifting buoy data (Rinaldi et al., 2010). When the Tyrrhenian meridional flow converges in the GoN, the surface circulation in its interior is characterized by a jet current (with a mean velocity of ~ 12 cm s^{-1}) oriented from the SE to the NW along the Bocca Piccola - Procida Channel axis (Figure 5b). The jet current axis separates the GoN circulation into two parts, as follows: east to the surface current describes an anticyclonic circulation, while on the west it is cyclonic. The patterns are in agreement with the previous *in situ* observations of De Maio et al. (1983).

The above description suggests obvious qualitative agreement between wind regimes and current patterns (with the exception of the *TYR* case study), and was further investigated and quantitatively assessed by performing a cross-correlation between winds and currents.

In order to have more than one wind data point in the area, we resorted to the Cross-Calibrated Multi-Platform (CCMP) surface wind velocities made available by the NASA Physical Oceanography Distributed Active Archive Center. The data are derived from ocean surface wind data from SSM/I, TMI, AMSR-E, SeaWinds on QuikSCAT, and SeaWinds on ADEOS-II, combined with conventional observations; and from a beginning estimate of the wind field using a variable analysis method. Wind fields were available from 1987-2010 every 6 hours with a 25 km spatial resolution (Ardizzone et al., 2009).

For each period, wind data were interpolated in space and time on the HF radar data grid. In order to estimate Ekman currents, a complex linear regression model was applied, as follows:

$$\boldsymbol{U} = \beta e^{i\vartheta}\boldsymbol{W} + error$$

where **U** and **W** are the radar current and CCMP are the wind velocities, expressed as complex numbers (**W** = w_1+iw_2), β is a real constant, and θ is an angle. β and θ represent the speed factor and the rotation angle of the Ekman currents with respect to the wind direction. Similar models have been applied to drifter data (e.g., by Niiler et al., 2003; Poulain et al., 2009; and Poulain et al., 2012) and also to radar data in the Kuroshio area (Tokeshi et al., 2007). The results of this analysis are summarized in Table 2. The Ekman currents estimated from the coastal radar were 1.3 to 2.0% of the wind speed, rotated to the right of the wind direction with an angle varying between 21° and 26°.

Table 2. Results of the analysis of the cross correlation between Ekman and total surface currents for the four case studies. See section 3 for an explanation. N represents the total number of data points over which the analysis was performed

Case study	Wind direction	Bexp(θ)	R^2 (%)	N
LND	NE	0.013exp(-21°i)	3	68734
SEA	SW	0.014exp(-25°i)	11	78995
BRZ	Breeze	0.020 exp(-23°i)	21	63907
TYR	NE	0.014exp(-26°i)	0.5	76355

The complex correlation coefficient, evaluated according to Kundu (1990), provided information on the correlation between currents and winds. In Table 2, the correlation is expressed in terms of the determination coefficient (R^2), which is the square of the complex correlation coefficient (Emery and Thomson, 2001). In the *LND* case study the Ekman current was responsible for 3% of the variance of surface currents measured by coastal radar. In the *SEA* case study the percentage rose to 11%, and in the *BRZ* case study to 21%, whereas in the *TYR* case study it was reduced to 0.5%.

The result confirms the qualitative discussion and indicates how the highest correlation occurs with a breeze, whereas the correlation is basically null when a strong Tyrrhenian coastal current develops. For the case of steady and strong winds (for the case studies *LND* and *SEA*) the correlation was half as high as that of the breeze case. For those cases, the locally forced circulation is apparently modulated by more complex dynamics. The difference between the *LND* and *SEA* case studies most likely rests in the fact that winds from the NE were distorted by the presence of Vesuvius, which has an influence on a portion, but possibly not the entire, basin.

4. TRACER TRANSPORT IN THE GULF OF NAPLES

The GoN represents an area of great interest to tourists and for commercial activities, but is extremely vulnerable (from a marine environment standpoint) due to the presence of several industrial sites along the coast, highly polluted river estuaries, and intense maritime traffic. For this reason, an understanding of the transport dynamics developing in the basin is important for implementing response strategies and procedures in cases of emergencies, whether they be represented by a pollution event, an oil spill, or a shipwreck.

Surface transport processes of passive tracers have been studied in the GoN by applying an oil spill model, the GNOME trajectory model (General N.O.A.A. Operational Modeling Environment) developed by the National Oceanic and Atmospheric Administration (NOAA) of the U.S.A.. GNOME is a mixed Lagrangian-Eulerian transport model that provides particle trajectory estimates by processing oceanographic as well as atmospheric data for a fixed geographic region (Beegle-Krause, 2001). GNOME offers three modes that differ from one another in the degree of control on the input parameters. In our study we used GNOME as a classic transport model in the diagnostic mode, and set all of the model data fields and parameters (Beegle-Krause, 2001). We considered a Lagrangian passive and conservative tracer moved by GNOME for an Eulerian current and wind field. Surface current fields were supplied to the model by the HF radar system operating within the GoN. HF radar current estimates present intrinsic uncertainties as compared to *in situ* measurements (e.g., Chapman et al., 1997; Ullman and Codiga, 2004). To account for this effect, we set a ± 15% error estimate in GNOME in both the along- and cross-current directions.

As an additional forcing mechanism contributing to transport processes ("mover", in GNOME jargon), we used hourly-averaged 10 m wind data collected by the DiSAm using an automatic weather station located on the urban littoral of Naples (Acton, see Figure 1). As discussed in section 2, since wind is a major driver of circulation in the GoN, its effect on circulation is already included in the surface current field detected by the radar system. However, in the simulations the direct effect of wind on the movement of a surface buoyant body, as could occur for an oil spill or for the case of a search and rescue simulation, was included. In GNOME this is accomplished by including the *windage* parameter, by including the Stokes drift and the momentum directly imparted by wind onto the particle (Engie and Klinger, 2007).

In addition to advection by surface currents and wind drift, a stochastic component to particle motion, in the form of a random walk (see, e.g., Csanady, 1980) parameterized by eddy diffusivity, was also included.

The relative effects of advection, windage, and diffusion were also studied in a parametric way by keeping the current constant and by allowing the wind and diffusivities to span the ranges reported in Table 3. In particular, for the wind field we used the actual value measured by the weather station, one tenth of the value, and also considered the case of a total absence of wind. We let the diffusivity range from zero to 10^6 cm^2 s^{-1} using 10^4 and 10^5 cm^2 s^{-1}. Worth noting, here, is that typical diffusivity values for dynamics with a spatial scale on the order of 1-10 km can be estimated to occur between 10^4 and 10^5 cm^2 s^{-1} (Okubo, 1971).

For the four case studies introduced in the previous sections, transport processes were numerically investigated using GNOME. Simulations of the trajectories of 10,000 particles were performed for each one-week period.

The study of transport processes in the GoN have largely focused on the properties of its most important sub-area immediately off the urban littoral (the Bay of Naples (see Figure 1)), in particular in regards to the effectiveness of its water renewal mechanisms. Therefore, particles have been deployed in the Bay and particle exchange between the Bay and the interior of the Gulf have been assessed in order to describe the effects of advection, diffusion, and wind in terms of two integral descriptors of transport within a semi-enclosed basin, as defined by Buffoni et al. (1997) for the normalized tracer quantity in the Bay *Q(t)* and the tracer residence time *T*.

Table 3. The forcings used for the parametric study. In the wind intensity column "v" represents the speed measured at the DiSAm station

WIND INTENSITY	DIFFUSIVITY($cm^2\ s^{-1}$)
0, v/10, v	0, 10^4, 10^5, 10^6

The normalized number of particles that, at a generic time (*t*) following deployment, were still located inside the release area (Bay of Naples) was estimated as follows:

$$Q(t) = \frac{N(t)}{N(0)}$$

where *N(t)* is the number of particles present at time *t* and *N(0)* is the pool of the originally launched tracers.

When applicable, the residence time, the time spent by a particle in the release area before exiting, was computed as follows:

$$T = \lim_{t \to \infty} T^*(t)$$

with:

$$T^*(t) = t\,Q(t) + \sum_{i=1}^{N_e(t)} \frac{t_{ei}}{N(0)}$$

where $N_e(T) = N(0) - N(t)$ is the number of particles that had already abandoned the deployment area at *t*, and t_{ei} represents the time taken by the i^{th} particle to first exit. Preliminary analysis indicated that when a particle exited the original domain it was not retained subsequent to the time period investigated, making the definition for a buffer zone (as outlined, e.g., by Falco et al., 2000) unnecessary.

Figures 6, 7, 8, and 9 display the behavior of Q(t) for all of the performed experiments, as well as for the final particle distribution in the AD case (see below) for the most realistic level of horizontal diffusion (10^4 cm^2 s^{-1}).

Given the number of different experiments performed (12 forcing combinations for four different case studies, leading to 48 simulations), in the following we focus our discussion on three forcing combinations for each case study. Thereafter, we briefly comment on the results contained in Table 4, which provides the values attained for the residence time (T) for all of the experiments.

In the description below, we define A as the case for which transport is only due to advection by surface currents (i.e. the wind and diffusion were set to zero). AD is defined as the case for which both advection and diffusion (with diffusivity set to 10^4 cm^2 s^{-1}) were present. ADW is the case for which wind was measured by the weather station in addition to advection and diffusion.

The LND case study (Figure 6)*:* The LND case study was characterized by a very effective renewal mechanism of Bay of Naples waters, and in all simulations the final concentration of the tracer particles in the bay did not exceed 4%. For the A condition all of the particles abandoned the release sector and remained afloat, with a T ~44 h. The cloud was split into two parts after ~3 days: one was advected by the coastal jet that rapidly brought particles toward the offshore sector of the GoN, while the other was transported to coastal sub-areas (Gulf of Castellammare) where local circulation entrapped the tracer.

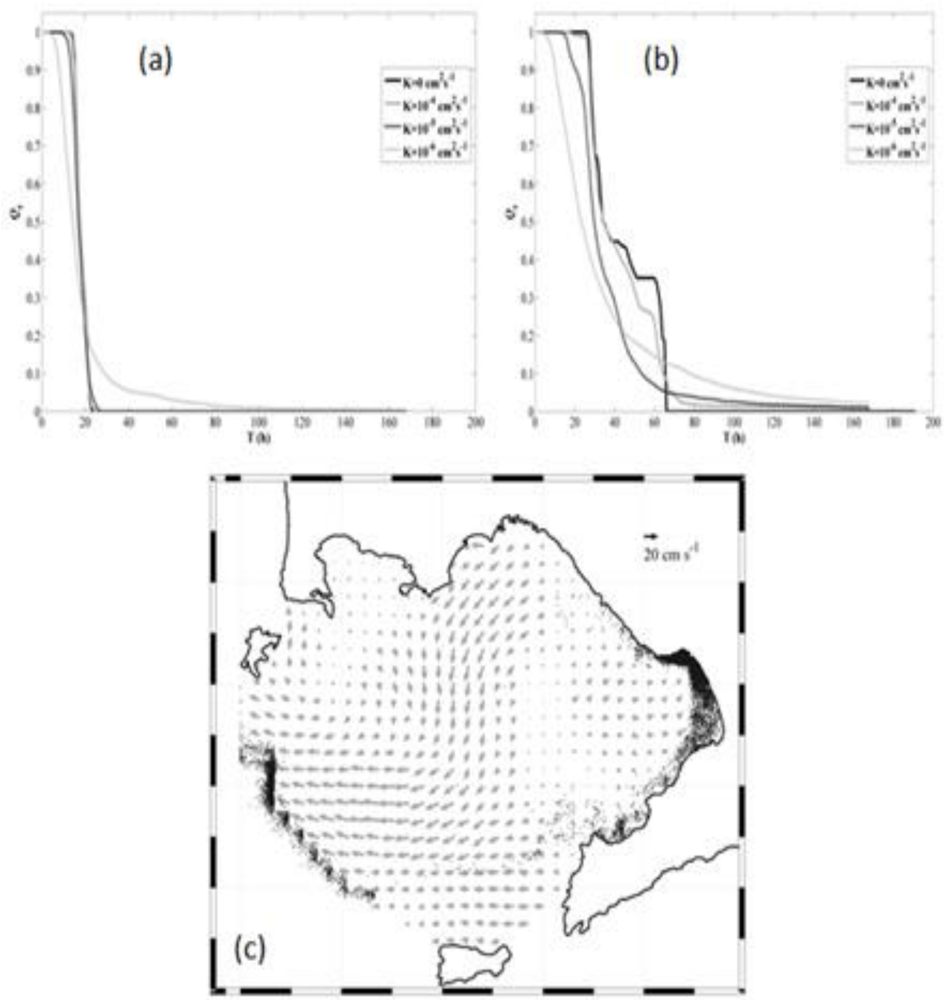

Figure 6. Results of the transport simulation relative to the LND case study: **(a)** Q(t) for null wind; **(b)** Q(t) for actual wind as measured by the Acton weather station; and **(c)** the final particle distribution for the case of null wind, with a diffusivity of $K=10^4$ cm^2 s^{-1}**.**

In the AD case, *T* was also ~44 h. Diffusion spread the cloud which, in this case, separated into two branches after ~3 days. One of the clouds entered the coastal jet and approached the "Bocca Grande". Approximately 1% of the particles were abandon by the GoN at the end of the simulation. In the second branch, the vast majority of the particles remained floating in the Gulf of Castellamare and in nearby areas, with a small percentage (12%) becoming stranded.

For the ADW condition all of the particles left the Bay of Naples, with a *T* of ~19 h. The wind rapidly pushed the tracer which, in ~4 days, reached the outer portion of the domain.

The SEA case study (Figure 7)*:* SW winds induced the strong retention of tracer particles within the Bay of Naples, and in all of the mover configurations *T* definitely exceeded the duration of the simulation. As compared to A, the effect of diffusion (AD) was manifest through the spreading of the cloud, with 24% of particles being stranded by the end of the simulation. When windage was accounted for (ADW), diffusion became the factor that massively (81%) pushed the tracer along the coast.

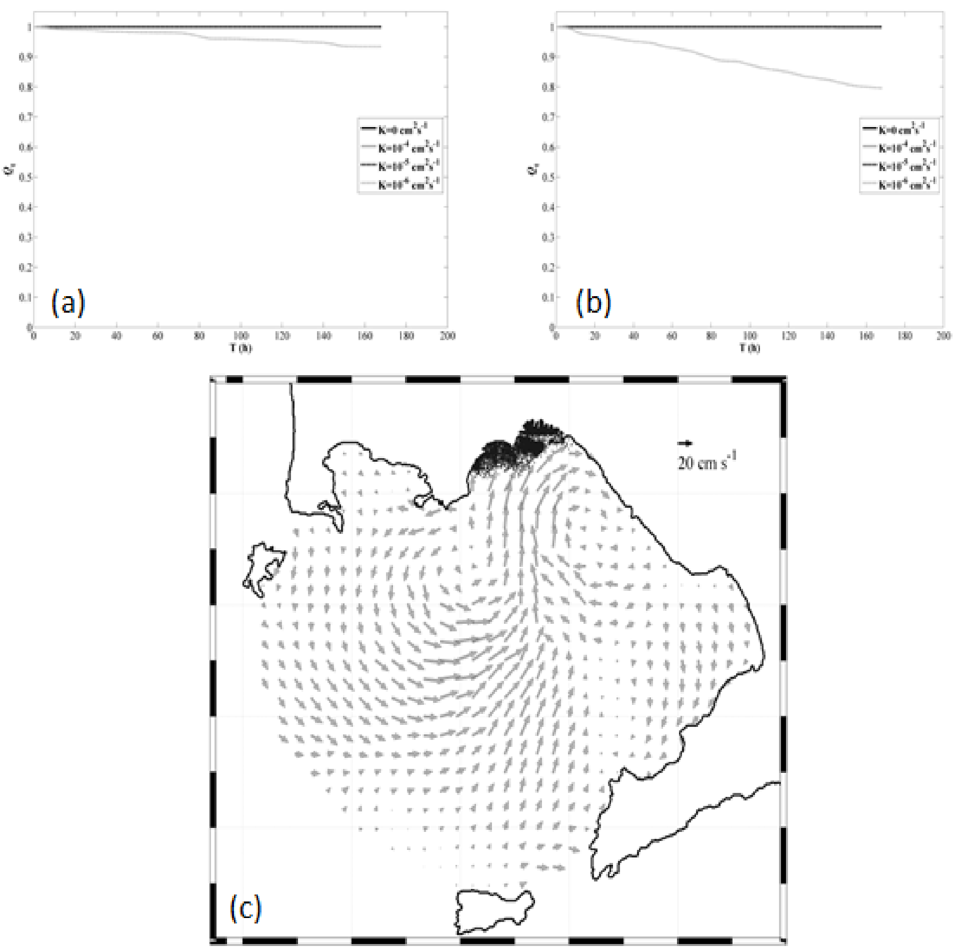

Figure 7. Results of the transport simulation relative to the SEA case study: **(a)** Q(t) for null wind; **(b)** Q(t) for actual wind as measured by the Acton weather station; and **(c)** the final particle distribution for the case of null wind, with a diffusivity of $K=10^4$ cm^2 s^{-1}**.**

The BRZ case study (Figure 8)*:* For the A condition all of the particles remained inside the release area. Within 24 hours, most of them were advected toward the coast by the sea breeze regime, where they became trapped in a small area without reaching open waters. In the AD case, particles became distributed inside the release area and were alternatively moved toward the coast or to open waters according to the breeze regime. By the 5th day of the simulation, some of the particles were stranded inside the launch sector (11%), while others were advected outside of the launch sector. Particles were transported by a meandering structure that retained them inside the GoN.

Similar results were reported for the ADW condition. The distinguishing feature was represented by a larger amount of beached particles inside the release area (26%).

The TYR case study (Figure 9)*:* For case A the tracer was first advected toward the boundary of the release sector within ~24 hours. Then it was divided into two small clusters. The first was transported by a coastward current until stopping in an area not sampled by the radar system. The second was advected toward the offshore sector. After roughly 5 days, a portion entered a coastal sub-area (Bay of Pozzuoli), whereas the remaining one crossed the Tyrrhenian jet and entered the cyclonic circulation on the left of the jet, approaching the “Bocca Grande”.

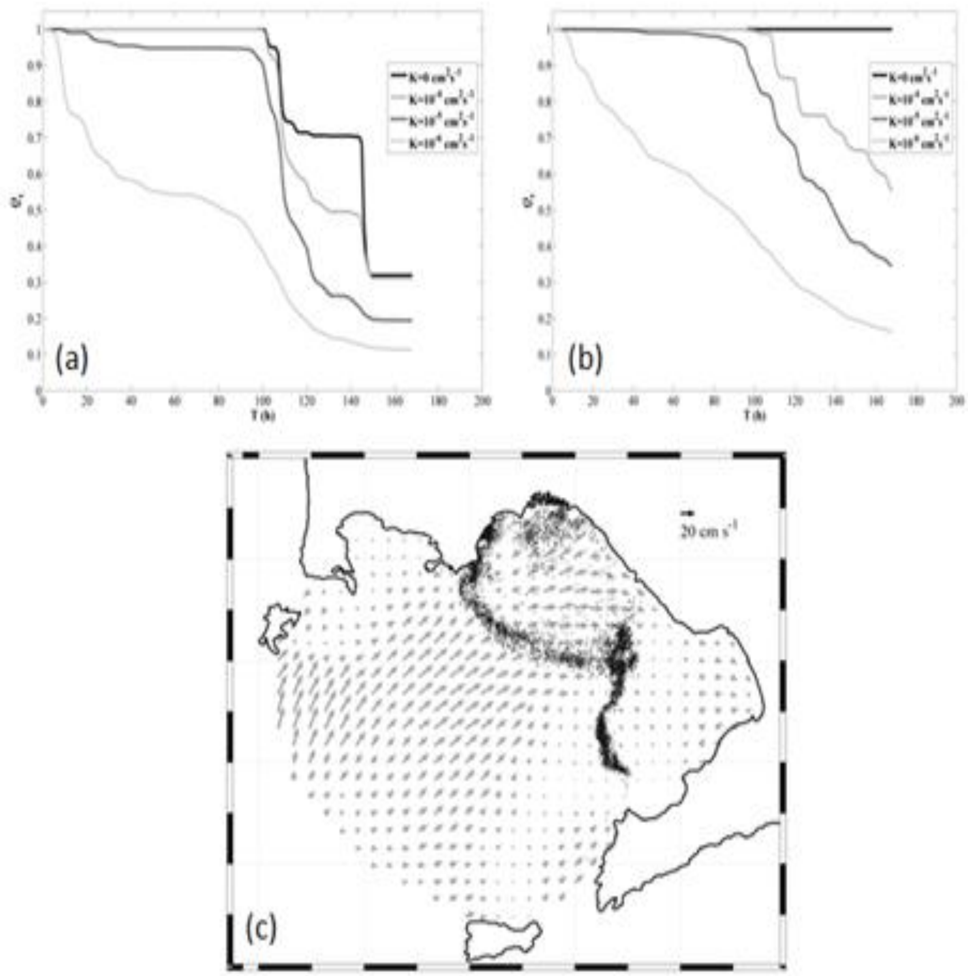

Figure 8. Results of the transport simulation relative to the BRZ case study: **(a)** Q(t) for null wind; **(b)** Q(t) for actual wind as measured by the Acton weather station; and **(c)** the final particle distribution for the case of null wind, with a diffusivity of $K=10^4\ cm^2\ s^{-1}$**.**

The overall dynamics were much more complex for the AD condition. When the cluster split after ~24 h, a first subset migrated toward the Bay of Pozzuoli. The second subset underwent more intricate dynamics. Part of it was first moved toward the coast. However, a meandering flow then transported most of the particles offshore. Therefore, another splitting was observed. Many of the tracers entered the Bay of Naples again and approached the littoral zone. Others, instead, crossed the Tyrrhenian jet and entered an offshore cyclonic gyre, being moved out of the GoN (22%). A similar scenario also occurred when windage was taken into account.

From the results for all of the simulations summarized in Table 4, we can see that in the *LND* case study, in which currents are strong and the dynamics relatively steady, the influence of diffusion on the tracer residence time in the Bay of Naples was small. On the contrary, the effect of windage strongly impacted estimates by enhancing water renewal by more than 2x in terms of *T*.

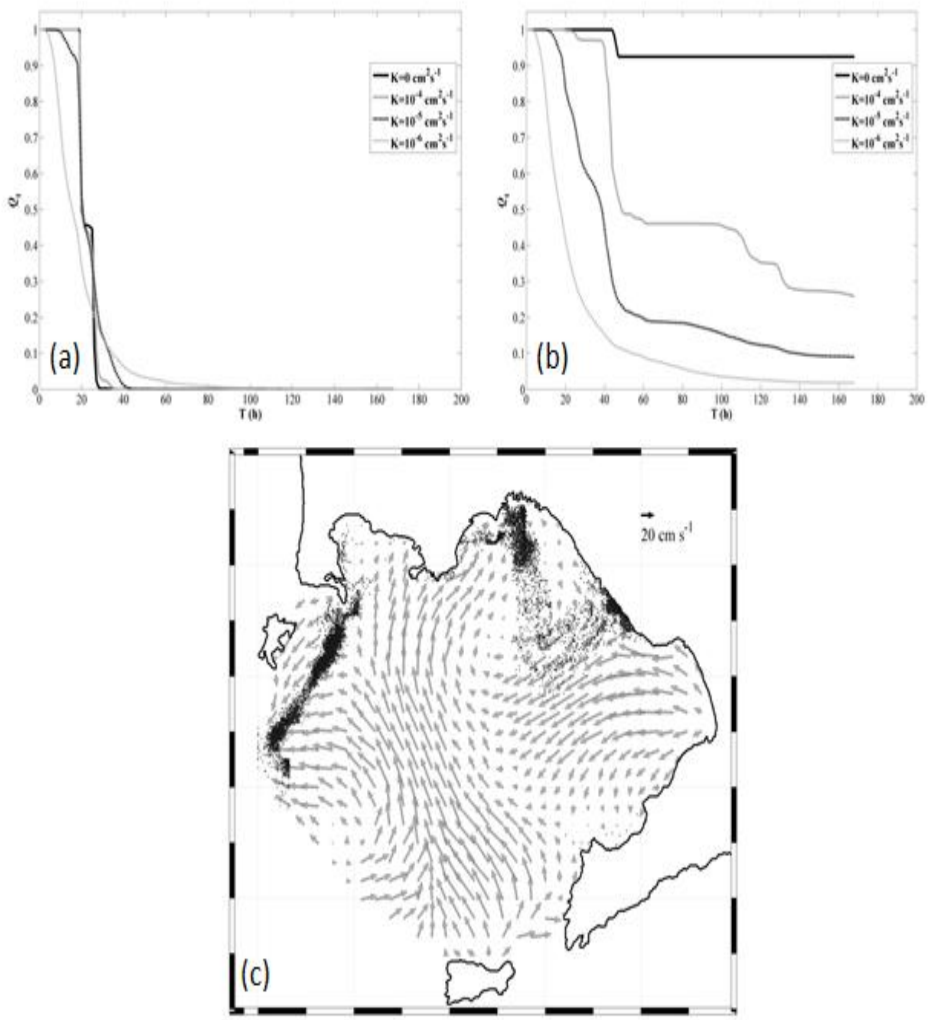

Figure 9. Results of the transport simulation relative to the TYR case study: **(a)** Q(t) for null wind; **(b)** Q(t) for actual wind as measured by the Acton weather station; and **(c)** the final particle distribution for the case of null wind, with a diffusivity of $K=10^4$ cm^2 s^{-1}**.**

Also, for the *SEA* case study that was characterized by strong currents and steady dynamics, diffusion did not make a significant difference. In this case this is true also for wind, obvious since its enhancing effect cannot be quantified in such a retentive (for the Bay of Naples) configuration.

For the *BRZ* case study that was dominated by a breeze regime, windage made only weak differences in the renewal mechanism of the Bay, and was strongly enhanced by the presence of diffusion that diminished *T* by a factor of two within the considered diffusivity range.

Diffusivity was also very important for the *TYR* case study, especially for weak or null wind. For the latter case, diffusivity decreased *T* by at least one order of magnitude. On the other hand, when windage was fully taken into account, given the fact that the dominating winds during that week blew from the NE, the results indicate a very strong enhancement of renewal, whether or not diffusion was present.

Table 4. The residence times, *T*, estimated in simulations for different forcing choices

Case Study LND			
Wind forcing diffusivity	*Calm*	*V/10*	*V*
0	44 hrs	32 hrs	19 hrs
$10^4\ cm^2s^{-1}$	44 hrs	33 hrs	19 hrs
$10^5\ cm^2s^{-1}$	37 hrs	31 hrs	18 hrs
$10^6\ cm^2s^{-1}$	36 hrs	33 hrs	19 hrs
Case Study SEA			
Wind forcing diffusivity	*Calm*	*V/10*	*V*
0	› 168 hrs	› 168 hrs	› 168 hrs
$10^4\ cm^2s^{-1}$	› 168 hrs	› 168 hrs	› 168 hrs
$10^5\ cm^2s^{-1}$	› 168 hrs	› 168 hrs	› 168 hrs
$10^6\ cm^2s^{-1}$	› 168 hrs	› 168 hrs	› 168 hrs
Case Study BRZ			
Wind forcing diffusivity	*Calm*	*V/10*	*V*
0	› 168 hrs	163 hrs	146 hrs
$10^4\ cm^2s^{-1}$	156 hrs	157 hrs	138 hrs
$10^5\ cm^2s^{-1}$	138 hrs	138 hrs	120 hrs
$10^6\ cm^2s^{-1}$	87 hrs	87 hrs	74 hrs
Case Study TYR			
Wind forcing diffusivity	*Calm*	*V/10*	*V*
0	› 168 hrs	45 hrs	23 hrs
$10^4\ cm^2s^{-1}$	92 hrs	52 hrs	23 hrs
$10^5\ cm^2s^{-1}$	52 hrs	55 hrs	23 hrs
$10^6\ cm^2s^{-1}$	27 hrs	27 hrs	19 hrs

5. Summary and Concluding Remarks

Here, the results of an investigation on surface currents, as well as the associated transport processes within the Gulf of Naples, as detected by a land-based remote sensing system, a HF coastal radar, are presented. Coastal radar provides a unique opportunity for obtaining a synoptic view of surface currents in relatively wide basins (with measurement ranges reaching 200 km for the case of long-range instrument configurations), with a high spatial and temporal resolution. For investigations of coastal dynamics, their characteristics make them almost irreplaceable for studies of pollutant transport or for search and rescue operations. For this reason, these systems are becoming more and more widespread along the world's coastlines (see, e.g., Harlan et al., 2010).

Synoptic measurements of surface currents allowed us to first identify typical circulation patterns within the GoN, strictly subordinate to local wind-stress or remote forcing. The relative importance of local and remote forcing was assessed by means of a cross-correlation analysis.

Wind in the area has been shown to mainly blow from the NE and SW quadrants, with the exception of summer which is dominated by a breeze regime. The three forcing configurations typically originate from surface circulation patterns, which have been investigated in dynamical terms, and with regard to the effectiveness of coastal water renewal, with a focus on the Bay of Naples - immediately off the urban littoral.

In the presence of NE winds, basin scale circulation develops a jet located in the central region of the GoN. The jet structure, directed offshore towards the Bocca Grande, typically induces cyclonic and anticyclonic circulations on a sub-basin scale. Also, in the southern region of the basin, surface currents are oriented along the wind direction. The resulting circulation promotes offshore-oriented transport from the coastal sector and prevents the import of particles from the offshore sector toward the Bay of Naples.

For SW winds, the GoN surface circulation is, on the whole, characterized by onshore dynamics. In the coastal areas of the basin, cyclonic and anticyclonic structures are formed, and support water recirculation processes, preventing the renewal of water masses. In the northern portion of the basin, surface circulation is more structured and presents an intense coastward oriented current. The area maintains a clear tendency to cyclonic rotation. Such surface dynamics enhance the retention of particles within the coastal area, as well as with an onshore particle flux from the interior of the Gulf.

In the breeze regime**,** the surface current direction closely follows the evolution of the wind direction. The entire pattern of surface circulation is seen to rotate clockwise, completing a 360° rotation in 24 hrs. The current pattern supports the gradual particle emptying of the coastal zone, while only a limited fraction of the particles released in the center of the Gulf reach the Bay of Naples.

In addition to locally forced regimes, the presence of a strong current at the outer boundary of the GoN may become a remote forcing, inducing a circulation in the interior that may be independent of the wind. In such a situation, Tyrrhenian water masses flow into the GoN and canalize through the Bocca Piccola forming a jet current oriented from SE to NW. The jet structure separates the GoN dynamics in two distinct sectors - east of the Tyrrhenian jet the surface current assumes an anticyclonic orientation, whereas on the west a cyclonic circulation develops. Both structures and the jet are minimally correlated with the wind direction, indicating that such dynamics are not driven by local wind forcing but are instead influenced by the Southern Tyrrhenian Winter circulation. The Tyrrhenian-driven circulation is favourable in regards to the renewal of Bay of Naples surface waters.

The relative importance of the different factors affecting surface transport in the area was assessed by examining the residence time of tracer particles using different simulations for an assortment of movers - strong and steady winds also led to strong and steady current patterns yielding residence times that were not sensitive to the effect of diffusion. On the contrary, transport processes in the case of a breeze regime were strongly impacted by diffusivity, and the case of remote forcing was seen to strongly depend on additional windage effects.

Our work reaffirms the unique possibilities provided by current measurements obtained using remote sensing instruments such as land-based HF coastal radars, that allow a synoptic view that is crucially important for studying both local dynamics and transport processes in coastal areas. These systems may play a leading role in operational oceanography networks – as recently demonstrated on the occasion of the environmental catastrophic event of the Deepwater Horizon oil spill in the Gulf of Mexico during the spring of 2010, making them invaluable to decision makers and stakeholders in devising specific policies for the management of coastal zones.

ACKNOWLEDGMENTS

The Dipartimento di Scienze per l'Ambiente of the "Parthenope" University operates the HF radar system on behalf of the AMRA consortium (formerly CRdC AMRA), a Regional Competence Center for the Analysis and Monitoring of Environmental Risks. Our radar remote sites were hosted by the ENEA centre of Portici, the "Villa Angelina Village of High Education and Professional Training" and "La Villanella" resort in Massa Lubrense, and the Fincantieri shipyard in Castellammare di Stabia, whose hospitality is gratefully acknowledged. Our work was partly funded by the MED TOSCA project, co-financed by the European Regional Development Fund, by the PROMETEO project, and funded by the Campania Region. Preparatory work was carried out in the framework of the EU Interreg III B Archimed CORI (the Prevention and Management of Sea Originated Risk to the Coastal Zone) project, and the Italian MIUR funded VECTOR project (subtasks 4.1.5 and 4.1.6). Partial support from the Procura della Repubblica (Public Prosecutor's office) of Torre Annunziata is also acknowledged.

We thank Jeffrey D. Paduan and Michael S. Cook for providing the OMA routines. Jeffrey D. Paduan's advice on several issues related to the coastal radar setup and data processing are also gratefully acknowledged. Discussions with Pierre-Marie Poulain helped improve estimates of Ekman currents. Gennaro Bianco is thanked for providing Acton wind data, and Alessandro Mercatini and Pasquale Mozzillo are thanked for supportive collaboration.

The GNOME package is freely available from NOAA's Office of Response and Restoration.

REFERENCES

Ardizzone, Atlas, Hoffman, Jusem, Leidner and Moroni.(2009). New multiplatform ocean surface wind product available.EOS Transactions American Geophysical Union. 90, 231.

Artale, Astraldi, Buffoni and Gasparini.(1994). Seasonal variability of gyre-scale circulation in the Northern Tyrrhenian Sea. *Journal of Geophysical Research.* 99 (C7), 14127-14137.

Barrick and Lipa. (1986). An evaluation of least-squares and closed-form dual-angle methods for CODAR surface-current applications. *IEEE Journal of Oceanic Engineering.* OE-11, 322-326.

Barrick, Evans and Weber. (1977). Ocean surface currents mapped by radar. *Science.* 198, 138-144.

Beegle-Krause. (2001) General NOAA Oil Modeling Environment (GNOME): a new spill trajectory model. In *IOSC 2001 Proceedings*; Mira Digital Publishing, Inc.: Tampa, FL, pp 865-871.

Buffoni, Falco, Griffa and Zambianchi. (1997). Dispersion processes and residence times in a semi-enclosed basin with recirculating gyres: an application to the Tyrrhenian Sea. *Journal of Geophysical Research.* 102 (C8), 699-713.

Chapman, Shay, Graber, Edson, Karachintsev, L. and Ross. (1997). On the accuracy of HF radar surface current measurements: intercomparisons with ship-based sensors. *Journal of Geophysical Research.* 102 (C8), 18737-18748.

Cianelli, Uttieri, Buonocore, Falco, Zambardino and Zambianchi. (2012) Dynamics of a very special Mediterranean coastal area: the Gulf of Naples. In *Mediterranean Ecosystems: Dynamics, Management and Conservation;* Williams (Ed.); Nova Science Publishers, Inc.: New York, pp. 129-150.

Csanady. (1980). *Turbulent Diffusion in the Environment;* D. Reidel Publishing Company: Dordecht, pp 260.

Dahlin, Flemming, Nittis and Petersson. (2003). *Building the European Capacity in Operational Oceanography*. Elsevier Oceanography Series, Vol. 69; Elsevier: Amsterdam, pp 714.

De Maio, Moretti, Sansone, Spezie and Vultaggio.(1983). Dinamica delle acque del Golfo di Napoli e adiacenze. *Risultati ottenuti dal* 1977 al 1981. Annali, Istituto Universitario Navale - Napoli. LI, 1-58.

De Maio, Moretti, Sansone, Spezie and Vultaggio. (1985). Outline of marine currents in the Bay of Naples and some considerations on pollutant transport.Il *Nuovo Cimento*. 8C, 955-969.

Emery and Thomson. (2001). *Data Analysis Methods in Physical Oceanography;* Elsevier: Amsterdam, pp 654.

Engie and Klinger. (2007). Modeling passive dispersal through a large estuarine system to evaluate marine reserve network connections. *Estuaries and Coasts*. 30, 201-213.

Falco, Griffa, Poulain and Zambianchi.(2000). Transport properties in the Adriatic Sea as deduced from drifter data. *Journal of Physical Oceanography*. 30, 2055-2071.

Flemming, Vallerga, Pinardi, Behrens, Manzella, Prandle and Stel.(2002). *Operational Oceanography - Implementation at the European and Regional Scales*. Elsevier Oceanography Series, Vol. 66; Elsevier: Amsterdam, pp 572.

Gravili, Napolitano and Pierini. (2001). Barotropic aspects of the dynamics of the Gulf of Naples (Tyrrhenian Sea). *Continental Shelf Research.* 21, 455-471.

Grieco, Tremblay and Zambianchi. (2005). A hybrid approach to transport processes in the Gulf of Naples: an application to phytoplankton and zooplankton population dynamics. *Continental Shelf Research*. 25, 711-728.

Harlan, Terrill, Hazard, Keen, Barrick, Whelan, Howden and Kohut. (2010). The integrated ocean observing system high-frequency radar network: status and local, regional, and national applications. *Marine Technology Society Journal.* 44, 122-132.

Krivosheya and Ovchinnikov. (1973). Peculiarities in the geostrophic circulation of the waters of the Tyrrhenian Sea. *Oceanology*. 13, 822-827.

Kundu. (1990). *Fluid Mechanics*; Academic Press: San Diego, pp 730.

Lekien, Coulliette, Bank and Marsden. (2004). Open boundary modal analysis: interpolation, extrapolation, and filtering. *Journal of Geophysical Research.* 109, C12004.

Lipphardt, Kirwan, Grosch, Lewis and Paduan.(2000). Blending HF radar and model velocities in Monterey Bay through normal mode analysis. *Journal of Geophysical Research.* 105 (C2), 3425-3450.

Menna, Mercatini, Uttieri, Buonocore and Zambianchi. (2007). Wintertime transport processes in the Gulf of Naples investigated by HF radar measurements of surface currents. Il *Nuovo Cimento*. 30 C, 605-622.

Millot.(1999). Circulation in the Western Mediterranean Sea. *Journal of Marine Systems.* 20, 423-442.

Moretti, Spezie and Vultaggio. (1983). Sub-inertial waves observed in the Gulf of Naples. *Rapports de la Commission Internationale pour l'Exploration Scientifique de la Mer Méditerranée*. 28, 151-154.

Moretti, Sansone, Spezie, Vultaggio and De Maio. (1976-1977). Alcuni aspetti del movimento delle acque del Golfo di Napoli. Annali, Istituto Universitario Navale - Napoli. XLV-XLVI, 207-217.

Niiler, Maximenko, Panteleev, Yamagata and Olson. (2003). Near-surface dynamical structure of the Kuroshio Extension. *Journal of Geophysical Research.* 108, 3193.

Okubo.(1971). Oceanic diffusion diagrams. *Deep Sea Research*. 18, 789-802.

Paduan and Cook. (1997). Mapping surface currents in Monterey Bay with CODAR-type HF radar. *Oceanography*. 10, 49-52.

Paduan and Graber. (1997). Introduction to High-Frequency radar: reality and myth. *Oceanography*. 10, 36-39.

Pederson and Barrick.(2004). HF surface-wave radar-revisiting a solution for EEZ ship surveillance. *EEZ International*. 35-37.

Pedlosky. (1979). *Geophysical Fluid Dynamics*; Springer-Verlag: New York, pp 624.

Pierini and Simioli.(1998). A wind-driven circulation model of the Tyrrhenian Sea area. *Journal of Marine Systems*. 18, 161-178.

Poulain, Menna and Mauri. (2012). Surface geostrophic circulation of the Mediterranean Sea derived from drifter and satellite altimeter data. *Journal of Physical Oceanography*. 42, 973-990.

Poulain, Gerin, Mauri and Pennel. (2009). Wind effects on drogued and undrogued drifters in the Eastern Mediterranean. *Journal of Atmospheric and Oceanic Technology*. 26, 1144-1156.

Rinaldi, Buongiorno Nardelli, Zambianchi, Santoleri and Poulain. (2010). Lagrangian and Eulerian observations of the surface circulation in the Tyrrhenian Sea. *Journal of Geophysical Research*. 115 C04024.

Robinson. (2010). *Discovering the Ocean from Space - The Unique Applications of Satellite Oceanography;* Springer: London, pp 638.

Schmidt. (1986). Multiple emitter location and signal parameter estimation. *IEEE Transactions on Antennas and Propagation*. 34, 276-280.

Sherman. (1969). Synoptic Oceanography: Remote Sensing Studies of the Ocean; *DTIC Document: Fort Belvoir,* pp 20.

Sherman. (1978). An Overview of Remote Sensing Oceanogrpahy in the United States. *Proceedings of International Symposium on Remote Sensing of Environment (12th),* Held at Ann Arbor, MI. on Apr 20-26, 1978; National Technical Information Service: Alexandria, pp 14.

Teague, Vesecky and Fernandez. (1997). HF radar instruments, past to present. *Oceanography*. 10, 40-44.

Tokeshi, Ichikawa, Fujii, Sato and Kojima. (2007). Estimating the geostrophic velocity obtained by HF radar observations in the upstream area of the Kuroshio. *Journal of Oceanography*. 63, 711-720.

Ullman and Codiga. (2004). Seasonal variation of a coastal jet in the Long Island Sound outflow region based on HF radar and Doppler current observations. *Journal of Geophysical Research*. 109, C07S06.

Uttieri, Cianelli, Buongiorno Nardelli, Buonocore, Falco, Colella and Zambianchi. (2011). Multiplatform observation of the surface circulation in the Gulf of Naples (Southern Tyrrhenian Sea). *Ocean Dynamics*. 61, 779-796.